ORL

Smell and Taste Corner

ORL 2024;86:1–12
DOI: 10.1159/000532077

Received: June 8, 2022
Accepted: July 11, 2023
Published online: August 22, 2023

Anterior Skull Base Abnormalities in Congenital Anosmia

Xiaoguang Yan[a] Hakim Benkhatar[b] Yun-Ting Chao[a, c, d]
Charalampos Georgiopoulos[e] Thomas Hummel[a]

[a]Smell and Taste Clinic, Department of Otorhinolaryngology, TU Dresden, Dresden, Germany; [b]Department of ENT and Head and Neck Surgery, Versailles Hospital, Le Chesnay-Rocquencourt, France; [c]Division of Rhinology, Department of Otorhinolaryngology-Head and Neck Surgery, Taipei Veterans General Hospital, Taipei, Taiwan; [d]Institute of Brain Science, National Yang Ming Chiao Tung University, Taipei, Taiwan; [e]Department of Radiology and Department of Medical and Health Sciences, Linköping University, Linköping, Sweden

Keywords
Anterior skull base · Morphology · Isolated congenital anomia · Magnetic resonance imaging

Abstract
Introduction: The structures of the skull and the brain are related to each other. Prior work in individuals with isolated congenital anosmia (ICA) showed that these individuals were characterized by olfactory bulb (OB) defects. The aim of this study was to compare the morphological pattern of the anterior skull base surrounding the OB between individuals with ICA and normosmic controls. We meant to investigate whether these features can help distinguish abnormalities from normal variation. ***Methods:*** We conducted a retrospective study to acquire T2-weighted magnetic resonance images from individuals diagnosed with ICA (n = 31) and healthy, normosmic controls matched for age and gender (n = 62). Between both groups, we compared the depth and width of the olfactory fossa, the angle of the ethmoidal fovea, as well as the angle of the lateral lamella of the cribriform plate. Within the ICA group, we further performed subgroup analyses based on the presence or absence of the OB, to investigate whether the morphology of the anterior skull base relates to the presence of OBs. The diagnostic performance of these parameters was evaluated using receiver operating characteristic analysis. ***Results:*** Individuals with ICA exhibited a flattened ethmoid roof and shallower olfactory fossa when compared to controls. Further, the absence of the OB was found to be associated with a higher degree of flattening of the ethmoid roof and a shallow olfactory fossa. We reached the results in the following areas under the receiver operating characteristic curves: 0.80 – angle of fovea ethmoidalis, 0.76 – depth of olfactory fossa, 0.70 – angle of lateral lamella of the cribriform plate for significant differentiation between individuals with ICA and normosmic controls. ***Conclusion:*** Individuals with ICA exhibited an unusual anterior skull base surrounding the OB. This study supports the idea of an integrated development of OB and anterior skull base. Hence, the morphological pattern of the anterior skull base surrounding the OB helps distinguish individuals with ICA from normosmic controls and may therefore be useful for the diagnosis of ICA, although it is certainly not an invariable sign of congenital anosmia.

Introduction

The intimate structural relationship between the skull and the brain has long been recognized in both evolutionary biology and clinical medicine. Research has consistently shown skull-brain morphological integration during hominin evolution [1, 2]. Skull development is

karger@karger.com
www.karger.com/orl

Correspondence to:
Xiaoguang Yan, xiaoguang.yan@outlook.com

Karger

highly coordinated. Unique changes in skull morphology, including a domed cranial vault, highly flexed cranial base, and retracted facial skeleton, are believed to be a direct result of a dramatic increase in brain size [3, 4]. Data by Trygve and his colleagues obtained in a European population suggested a tight correspondence between skull and brain morphologies [5]. In fact, skull malformations (e.g., craniosynostosis) and brain malformations (e.g., holoprosencephaly) can affect skull development and brain growth and vice versa.

The olfactory bulb (OB), located at the base of the anterior cranial fossa, is the critical first relay of the olfactory system. Congenital absence of the OB may co-occur with other brain malformations, for example, holoprosencephaly, which is the most common abnormality of brain development affecting the forebrain and the facial features in live-born infants [6]. OB defect can also present as an isolated finding or as a component of chromosomopathies (e.g., CHARGE syndrome) or endocrinopathies (e.g., Kallmann syndrome) [7, 8]. What's more, the absence of OBs occurs frequently as an isolated finding.

OB defect largely is found in congenital anosmia, characterized by a complete lack of olfactory perception since birth and aplasia or hypoplasia of the OB [9]. Accordingly, congenital anosmia can be combined with other anomalies, with Kallmann syndrome being the best documented, or without evidence of other defects, termed isolated congenital anosmia (ICA). The estimated prevalence of ICA is between 1 in 2,000 and 1 in 8,000, and it is now thought to be the most common form of congenital anosmia [10–12]. Brain structural changes, such as reduced depth of the olfactory sulcus, regularly accompany OB defects and are considered a useful clinical indicator of congenital anosmia [13]. Structural alterations are not limited to the OB and the olfactory sulcus, as the entorhinal and piriform cortices appear to be thicker in congenital anosmia [14]. Given the close relationship between the skull and brain forms, it follows that the nearby skull may also differ in size and shape in individuals with OB defect. However, not much attention has been paid to changes of bony structures neighboring the OB due to the congenital factor, even though alterations of the anterior skull base have been reported in Kallmann syndrome [15].

The anterior skull base consists of the cribriform plate and fovea ethmoidalis (FE), an extension of the frontal bone orbital plate, separating the anterior cranial fossa superiorly and paranasal sinuses ventrally. The lateral lamella joins the cribriform plate to the FE, forming the lateral wall of the olfactory fossa (OF). The configuration of the anterior skull base is highly variable. The depth of the OF was described and classified by Keros into three main types: Keros type 1 (<3 mm), type 2 (4–7 mm), and type 3 (8–16 mm) [16]. The FE can also vary considerably with intraindividual asymmetry. In fact, Lebowitz et al. [17] reported that 9.5% (19/200) computed tomographic (CT) scans show an asymmetry of the height of the FE.

To date, there has been no research investigating the relationship between an OB defect and the structure of the surrounding skull base in the context of ICA. The presence of skull base anomalies in ICA might contribute to the understanding of its pathogenesis; the existence or lack of a structural association between skull base and OB may also provide more information as to the etiology of this process. Our hypothesis was that the morphology of the anterior skull base, as measured in terms of the depth as well as width of the OF, the angle of the lateral lamella of the cribriform plate (LLCP), and the angle of the FE, is different between ICA participants and healthy controls. We further hypothesized that in ICA, the morphology of the anterior skull base is correlated to OB abnormalities and that the morphological parameters are correlated with each other.

The aim of this study was to identify and compare the morphological pattern of the anterior skull base surrounding the OB between individuals with ICA and normosmic controls using magnetic resonance imaging (MRI). Specifically, we aimed to investigate the diagnostic value of the surrounding skull base structure and its relationship with the OB defects, which has not been fully explored in previous studies. By using MRI as the imaging modality, we aimed to provide a more detailed and accurate assessment of these abnormalities, which could potentially lead to improved diagnostic and treatment strategies for patients with ICA.

Materials and Methods

Study Design and Setting

This was a retrospective study conducted by reviewing medical records of patients who received treatment in the Smell and Taste Clinic of the Department of Otorhinolaryngology at TU Dresden. All participants provided written informed consent. They participated in studies that had been approved by the Ethics Committee at the Medical Faculty at the "Technische Universität Dresden".

Participants

Inclusion Criteria

Congenital anosmia was diagnosed according to the "position paper on olfactory dysfunction" [18] based on (1) detailed structured medical history; participants reported that they never

experienced any olfactory perception [19]; (2) psychophysical examination was assessed with the extended Sniffin' Sticks olfactory test (Burghart, Wedel, Germany) with participants' TDI (threshold-discrimination-identification) score in the range of anosmia (score ≤16) [20]; (3) electrophysiological measurements; participants did not exhibit an EEG response following olfactory stimulation [21]; (4) MRI; the OB or olfactory tract was aplastic or hypoplastic (according to the literature, ICA, when both OB and olfactory tract are normal, is very rare) [9]. Randomly selected healthy controls with no known history of olfactory dysfunction were recruited by advertisement and were matched to the participants by age (±2 years) and gender.

Exclusion criteria were based on the following: (1) signs and symptoms of different conditions possibly causing anosmia (severe chronic rhinosinusitis, traumatic brain injury, etc.); (2) altered anatomy of the anterior skull base or paranasal sinus due to iatrogenic causes or other pathology, e.g., tumors; (3) obscured ethmoid sinus pathology; (4) congenital anosmia combined with other anomalies, e.g., Kallmann syndrome, CHARGE syndrome.

Data Sources/Measurement

MRI Acquisition

MRI was performed using a 3-Tesla scanner (model Prisma; Siemens, Erlangen, Germany) and a 32-channel coil. Images were acquired with T2-weighted sequence, covering the anterior and middle segments of the head. The scanning parameters were: 30–46 slices, slice thickness 1 mm, no gap, echo time = 78 ms, repetition time = 1,500 ms, flip angle = 150°, field of view matrix = 256 × 320.

Structural Assessment

For delineating and measuring the anterior skull base, we used ITK-SNAP, which provided tools to measure lengths and angles of anatomical structures. Measurements were made in the coronal plane of the posterior tangent through the eyeballs [12]. The following parameters were recorded on both sides: (1) depth of the OF (in mm), measured as the vertical height of the OF and classified by the Keros' classification system into type 1 (depth 1–3 mm), type 2 (depth 4–7 mm), or type 3 (depth more than 8 mm) [16] (asymmetry in the depth [difference of more than 1 mm] between the right and left OF was also examined); (2) width of the OF (in mm), defined as the distance between the crista galli and the lateral wall of the OF through the depth of the OF medially and perpendicularly; (3) angle of the LLCP (in degrees), measurement was calculated at the angle formed by the LLCP and the horizontal line drawn through the cribriform plate. This was further classified into 3 classes depending on the hypothetical risk of iatrogenic injuries: class I (>80°, low risk), class II (45–80°, medium risk), and class III (<45°, high risk) [22]; (4) angle of the FE (in degrees), calculated as the angle formed by the FE and LLCP; (5) depth of the olfactory sulcus (Fig 1). For describing the status of OB concerning the development, we divided it into 2 phenotypes: ICA with OB present and ICA with the absence of OB.

Statistical Analysis

SPSS version 26 (SPSS Inc., IL, USA) was used for data analysis; graphical visualization was performed using GraphPad Prism 9.3.1 (GraphPad Software, Inc., La Jolla, CA, USA). Descriptive statistics were performed for all study participants. Student's *t*-test and χ^2 were used for comparisons between individuals with ICA and healthy controls. Receiver operating characteristic (ROC) curves were used to establish sensitivity and specificity of the depth of respective deepest OF, angle of respective largest LLCP, angle of respective largest FE. The optimal cutoff values were chosen based on the highest Youden index (sensitivity + specificity − 1). Cutoff values with the highest Youden index (optimal combination of sensitivity and specificity) have the least amount of overlap between groups, representing a clinically relevant cutoff. The area under the ROC curve was used to quantify diagnostic accuracy of these measurements. The association between measurements was estimated through Pearson's correlation coefficient. We further compared the measurements between individuals with ICA regarding the absence or presence of OB. p value <0.05 was considered statistically significant.

Results

Participants

We included a total of 93 participants: 31 individuals diagnosed with congenital anosmia (21 women; age 17–75 years, mean age 48.7 ± 16.8 years) and 62 healthy controls (42 women; age 18–76 years, mean age 48.1 ± 17.3 years), matched in terms of gender and age (Table 1). No significant differences were found between the ICA group and the control group in terms of age ($t = 0.16$, $p = 0.87$) and gender distribution ($p > 0.999$).

Smell Assessment for ICA and Healthy Participants

By comparing TDI scores, the smell function of ICA participants (11.4 ± 3.4, range: 2.0–16.0) was significantly lower than that of healthy controls (34.4 ± 4.1, range: 24.5–41.75) ($t = 26.77$, $p < 0.001$).

Comparison between ICA and Healthy Participants

A total of 93 MR slices (186 sides) were evaluated.

Depth of the OF

In ICA participants, the mean depth of the OF was 3.5 ± 1.5 mm (range: 1.3–8.0 mm) on the left side and 3.4 ± 1.4 mm (range: 1.3–7.0 mm) on the right side. In controls, the mean depth of the OF was significantly deeper (4.9 ± 1.6 mm (range: 2.4–8.6 mm) on the left side and 4.7 ± 1.6 mm (range: 1.9–7.6 mm) on the right side) (left: $t = 3.95$, $p < 0.001$; right: $t = 3.79$, $p < 0.001$) (Fig. 2). No significant differences in the depth of the OF were observed between ICA with OB and control (left: $p = 0.15$; right: $p = 0.12$). The most common Keros type was type 1 (41/62, 66%) in ICA participants, followed by type 2 (20/62, 32%) and type 3 (1/62, 2%). This distribution of Keros type was significantly different in healthy controls (Keros type 1: 41/124, 33%; Keros type 2: 79/124, 63%; Keros type 3: 4/124, 3%) (left: $\chi^2 = 7.12$,

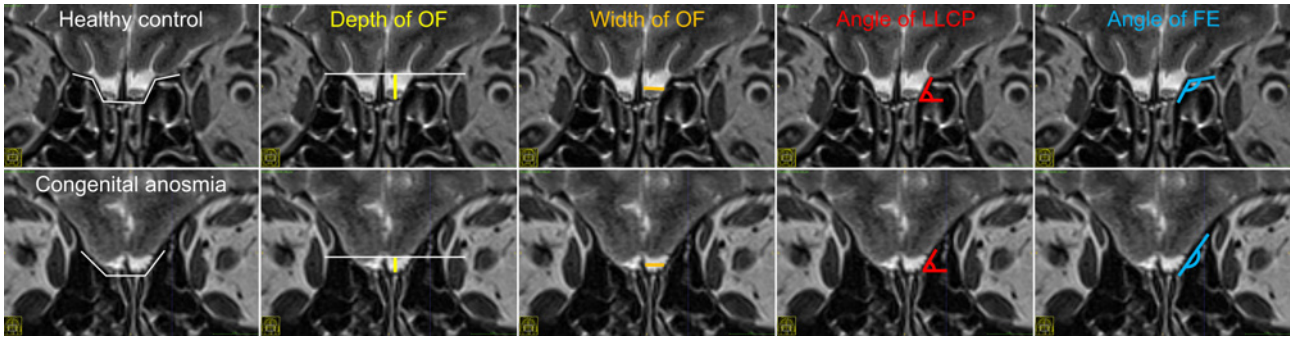

Fig. 1. "A representative MRI photo" for each of the MRI structural outcomes and the morphological pattern for both ICA participants ([51 years, female, TDI = 13] 5 images) and healthy controls ([72 years, female, TDI = 34.25] 5 images). Width of the OF (in mm, orange), depth of the OF (in mm, yellow), angle of the FE (in °, blue), angle of the LLCP (in °, red).

Table 1. Demographic, smell assessment, and radiologic characteristics

Characteristic	Congenital participants	Healthy control	Statistics	p value
Demographics				
Age, years, mean (SD)	48.7 (16.8)	48.1 (17.3)	$t = 0.16$	0.87
Gender	21F, 10M	42F, 20M	$\chi^2 = 0$	1
Development of OB				
Left	18A,13H *	–	–	–
Right	19A,12H	–	–	–
Depth of the OF, in mm				
Keros type, *N* (%)				
Kero type 1	41 (66)	41 (33)	$\chi^2 = 7.17$	$p < 0.001$
Kero type 2	20 (32)	79 (63)		
Kero type 3	1 (2)	4 (3)		
Smell assessment				
TDI, mean (SD)	11.7 (3.0)	34.4 (4.1)	$t = 26.77$	$p < 0.001$
Angle of the lateral lamella of cribriform plate				
Angle of LLCP classification, *N* (%)				
Class I	3 (4)	17 (14)	$\chi^2 = 11.95$	$p < 0.001$
Class II	23 (37)	76 (61)		
Class III	36 (58)	31 (25)		

Data are presented as means (standard deviation) or percentage (%). *A, aplasia; H, hypoplasia; TDI, threshold-discrimination-identification.

$p = 0.03$; right: $\chi^2 = 11.44$, $p = 0.001$). Asymmetry in the depth of the OF was reported in 10% (3/31) of ICA participants, which was significantly different from controls (19/62, 31%) ($\chi^2 = 5.03$, $p = 0.02$) (Table 1).

Width of the OF

The width of the left OF was smaller in individuals with ICA compared to healthy controls ($p = 0.03$). This difference was not significant for the right OF ($p = 0.21$)

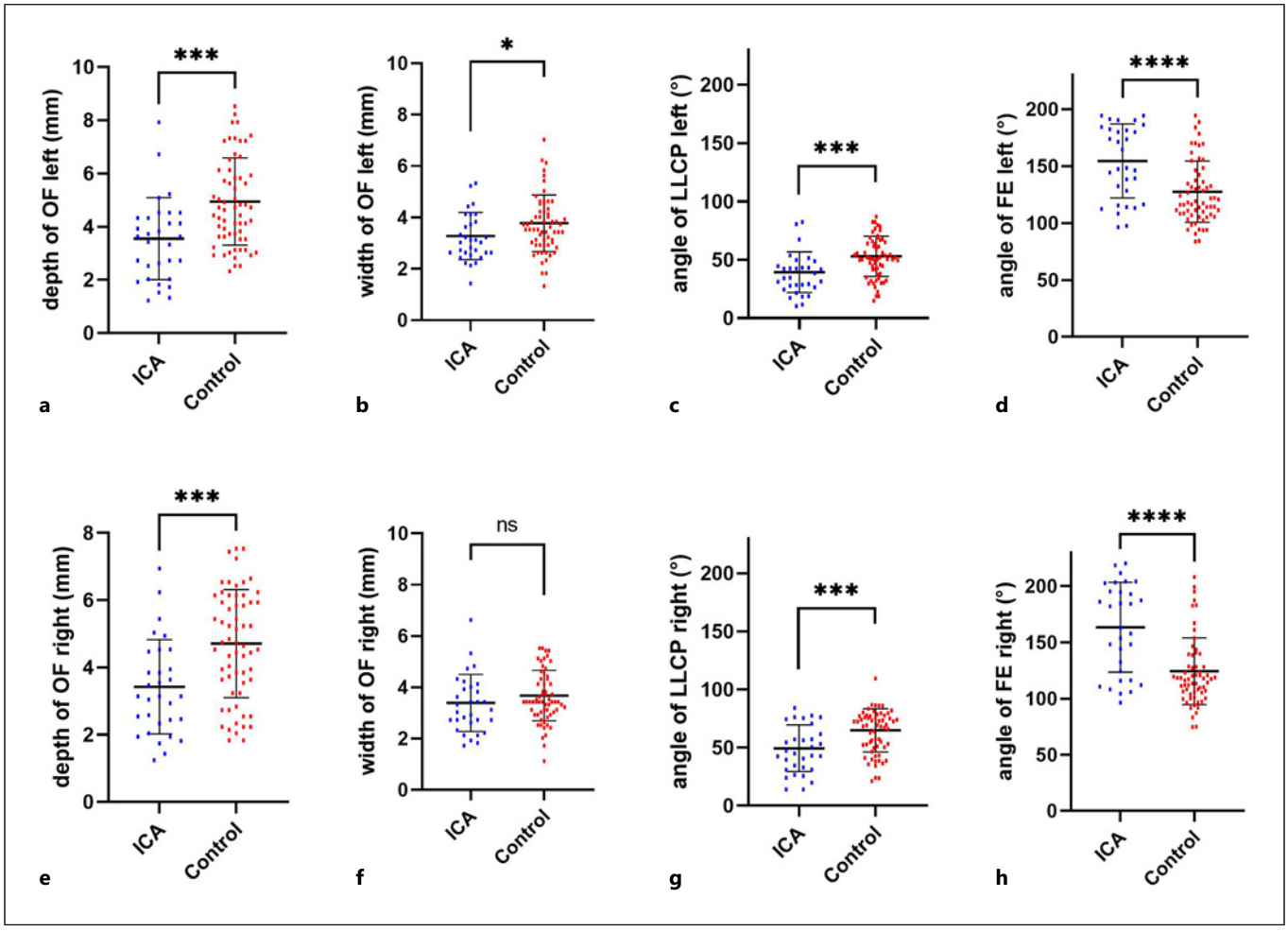

Fig. 2. Structures of the anterior skull base according to the groups and sides. **a**, **e** Mean of the depth of OF for ICA group and healthy control group at both sides. **b**, **f** Mean of the width of OF for ICA group and healthy control group at both sides. **c**, **g** Mean of angle of LLCP for ICA group and healthy control group at both sides. **d**, **h** Mean of angle of FE for ICA group and healthy control group at both sides. FE, fovea ethmoidalis; LLCP, lateral lamella of the cribriform plate; OF, olfactory fossa; L, left; R, right. *$p < 0.05$, **$p < 0.01$, ***$p < 0.001$, ****$p < 0.0001$, ns: $p > 0.05$.

(Fig. 2). No significant differences in the width of the OF were observed between ICA with OB and control (left: $p = 0.20$; right: $p = 0.99$).

Angle of the LLCP

In ICA participants, the mean degree of the angle of LLCP was 39.4 ± 17.5° (range: 12.0–84.0°) on the left side and 49.4 ± 20.0° (range: 15.6–85.8°) on the right side. These measures were significantly lower compared to controls (left: 53.0 ± 17.3°, range: 16.6–88.7°; right: 64.9 ± 18.6°, range: 22.9–111.2°) ($p < 0.001$) (Fig. 2). Relative to controls, the ICA with OB group had a significantly lower angle of LLCP at the left side ($p = 0.04$) but not at the right side ($p = 0.13$). Class III (<45°, high risk) was found in 58% (36/62) ICA participants, class I (>80°, low risk) in 4% (3/62) of cases, and class II (45–80°, medium risk) in 37% (23/62) of ICA participants. In healthy controls, while 25% (31/124) of class III, 14% (17/124) of class I, and 61% (76/124) of class II were found. The distribution of angle classification was different between ICA participants and controls ($\chi^2 = 11.95$, $p < 0.001$) (Table 1).

Angle of the FE

The angle of the FE on both sides was greater in individuals with ICA compared to healthy controls (all $p < 0.0001$) (Fig. 2). In the ICA with OB group, the angle of the right the FE was smaller compared to healthy controls ($p < 0.001$). This difference was not significant for the left angle of the FE ($p = 0.09$).

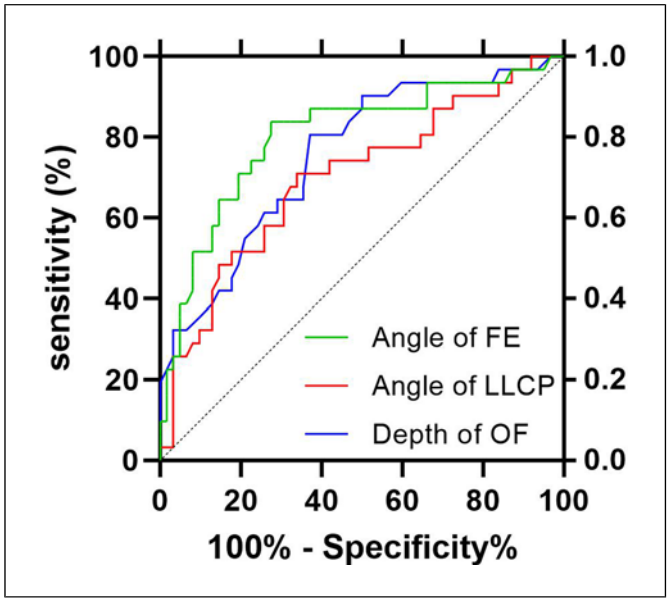

Fig. 3. Receiver operating characteristic (ROC) curve of FE (AUC = 0.73), angle of the LLCP (AUC = 0.73), depth of OF (AUC = 0.74), Keros types. when the cutoff values were determined by optimal test efficiency (defined by the highest Youden index), which shown 68–87% and 52–76% in terms of sensitivity and specificity, respectively. FE, fovea ethmoidalis; LLCP, lateral lamella of the cribriform plate; OF, olfactory fossa.

Predictors for Individuals with ICA

The ROC curve analysis of predictors for ICA is summarized (Fig. 3). The following parameters had good accuracy as predictors for individuals with ICA: angle of the FE (area under the receiver operating characteristic curve [AUC] = 0.80), angle of the LLCP (AUC = 0.70), depth of the OF (AUC = 0.76), Keros types (AUC = 0.65). The width of the OF had no ability to distinguish between individuals with ICA and healthy control ($p = 0.11$). Furthermore, the angle of the FE can distinguish ICA with OB from normosmic controls (AUC = 0.70, $p = 0.02$). Three cutoff values were determined from the ROC analyses for each parameter for predicting ICA: 1 for optimal test efficiency (defined by the highest Youden index) – which shown 71–84% and 63–73% in terms of sensitivity and specificity, respectively, 1 for maximum sensitivity (least number of false negatives), and 1 for maximal specificity (least number of false positives) (Table 2).

To further validate the accuracy of the clinical scenario application. We selected another dataset containing T2-weighted MRI images of 9 participants with congenital anosmia and 15 normosmic controls. Based on the methodology of this study, five ENT doctors, who were blinded to other clinical data, were asked to make a diagnosis visually based on morphological features of the anterior skull base only, with the OB and olfactory sulcus masked. The results showed that the diagnostic accuracy is more than random chance (rater 1: sensitivity [SE] = 0.89, specificity [SP] = 0.93; rater 2: SE = 0.67, SP = 1; rater 3: SE = 0.67, SP = 0.73; rater 4: SE = 0.89, SP = 0.80; rater 5: SE = 0.78, SP = 0.87).

Correlations of Skull Base Parameters

The results of the correlation analysis are reported in Figure 4. Correlation analysis revealed moderately positive correlations between angle of the LLCP and depth of the OF. Significant negative correlations were also found between the right-sided angle of the FE and angle of the LLCP (r between −0.63 and −0.74). To the contrary, no relevant correlation was found between width of the OF and depth of the OF.

Correlations between Olfactory Sulcus and Skull Base Parameters

The results of the correlation analysis are reported in Figure 4. In the ICA group, the left depth of OF correlated positively with the depth of the OF, angle of the LLCP, negatively with the right angle of the FE. A similar trend was observed at the right side. In the control group, the left depth of the OF showed a positive relationship with the left depth of OF, width of OF.

Relationship between Parameters and Presence of OB

ICA participants with the presence of OB showed a deeper OF (left: $t = 2.77$, $p = 0.01$; right: $t = 3.55$, $p = 0.001$) and larger left-sided angle of the LLCP ($t = 2.21$, $p = 0.04$) when compared with ICA participants without OB. Further, participants with presence of OB showed, on average, relatively greater width of the OF as well as the right-sided angle of the LLCP and lower FE. However, these differences were not statistically significant (Fig. 5).

Discussion

Key Finding

In participants with ICA, small or absent OBs are associated with morphological changes of the olfactory sulci, especially their depth [13]. Here, we investigated whether ICA is linked to altered skull structure by comparing the size and shape of the ethmoid roof and OF between individuals with ICA and matched control. In particular, the angle of the FE and LLCP as well as the depth and width of the OF were assessed. To our knowledge, this is the first investigation to suggest that

Table 2. Sensitivity, specificity of cutoff points of 4 morphological indices of anterior skull base for prediction of ICA

Variables	AUC (95% CI)	*p* values	Cutoff	Sensitivity (95% CI)	Specificity (95% CI)
Best depth of the OF	0.76 (0.65–0.86)	<0.001	<4.65 mm <2.25 mm <8.15 mm	0.81 (0.64–0.91) 0.19 (0.09–0.36) 1.00 (0.89–1.00)	0.63 (0.50–0.75) 1.00 (0.94–1.00) 0.01 (0–0.08)
Best angle of the lateral lamella of cribriform plate	0.70 (0.58–0.81)	<0.001	<64.0° <19.3° <86.9°	0.71 (0.53–0.84) 0.03 (0–0.16) 1.00 (0.89–1.00)	0.66 (0.54–0.77) 1.00 (0.94–1.00) 0.08 (0.03–0.18)
Best angle of the FE	0.80 (0.70–0.90)	<0.001	>148.6° >211.7° >95.6°	0.84 (0.67–0.93) 0.10 (0.03–0.25) 1.00 (0.89–1.00)	0.73 (0.60–0.82) 1.00 (0.94–1.00) 0.01 (0–0.08)
Best width of the OF	–	= 0.11	–	–	–

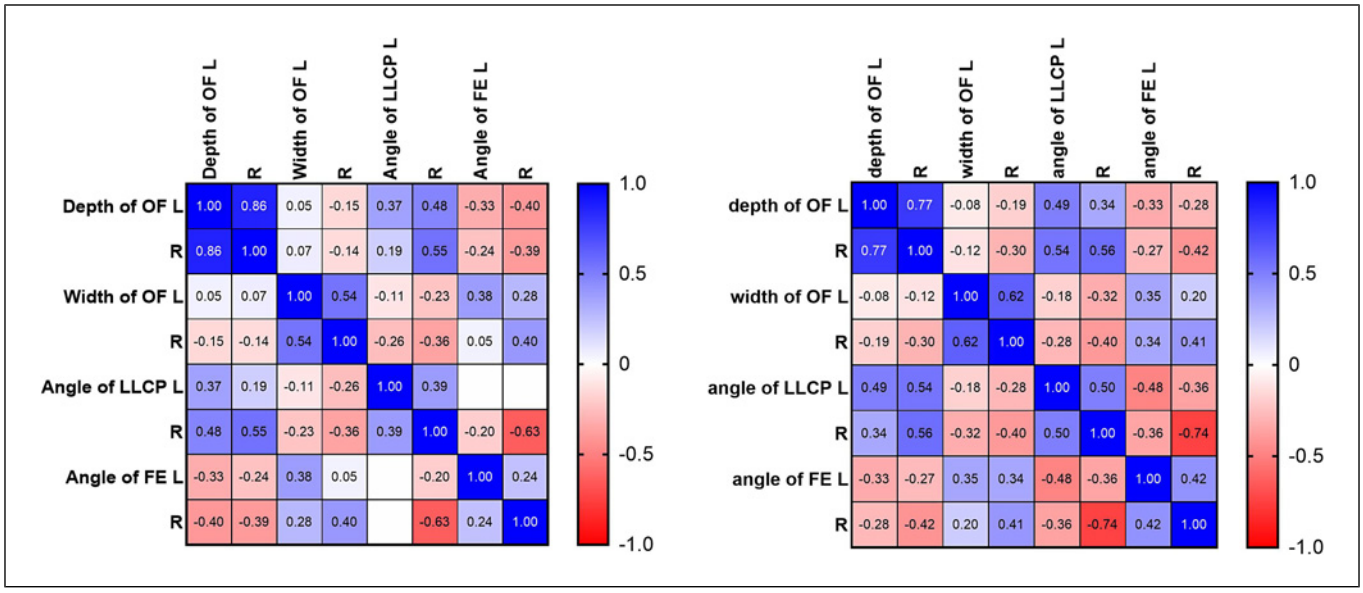

Fig. 4. Correlation matrix between measurements. The number represents Pearson's *r* values, positive correlations are displayed in blue and negative correlations in red color, color intensity is proportional to Pearson's *r* values. FE, fovea ethmoidalis; LLCP, lateral lamella of the cribriform plate; OF, olfactory fossa; OS, olfactory sulcus.

ICA is strongly linked to a "flattening" of the FE, shallow OF, and low angle of the LLCP compared with matched controls, with the three parameters also being correlated to each other. Indeed, the abnormalities of the ethmoid roof and OF seem to be related to the morphological status of OB. Our findings imply that ICA participants have an unusual pattern of structural variation in the anterior skull base. This pattern is characterized by a shallower OF and larger slope of the anterior skull base (Fig. 1).

Interpretation

The present results suggest that morphological changes in the anterior skull base are a clinical indicator of ICA. For example, the depth of the OF had the ability to differentiate ICA from healthy participants. Indeed, the optimal cutoff point of less than 2.25 mm depth of the OF was demonstrated to exhibit a specificity of 100%. Several studies investigated the normal depth of OF and corresponding distribution of Keros type. Elwany et al. [23] evaluated 300 participants and found Keros type II to be the most

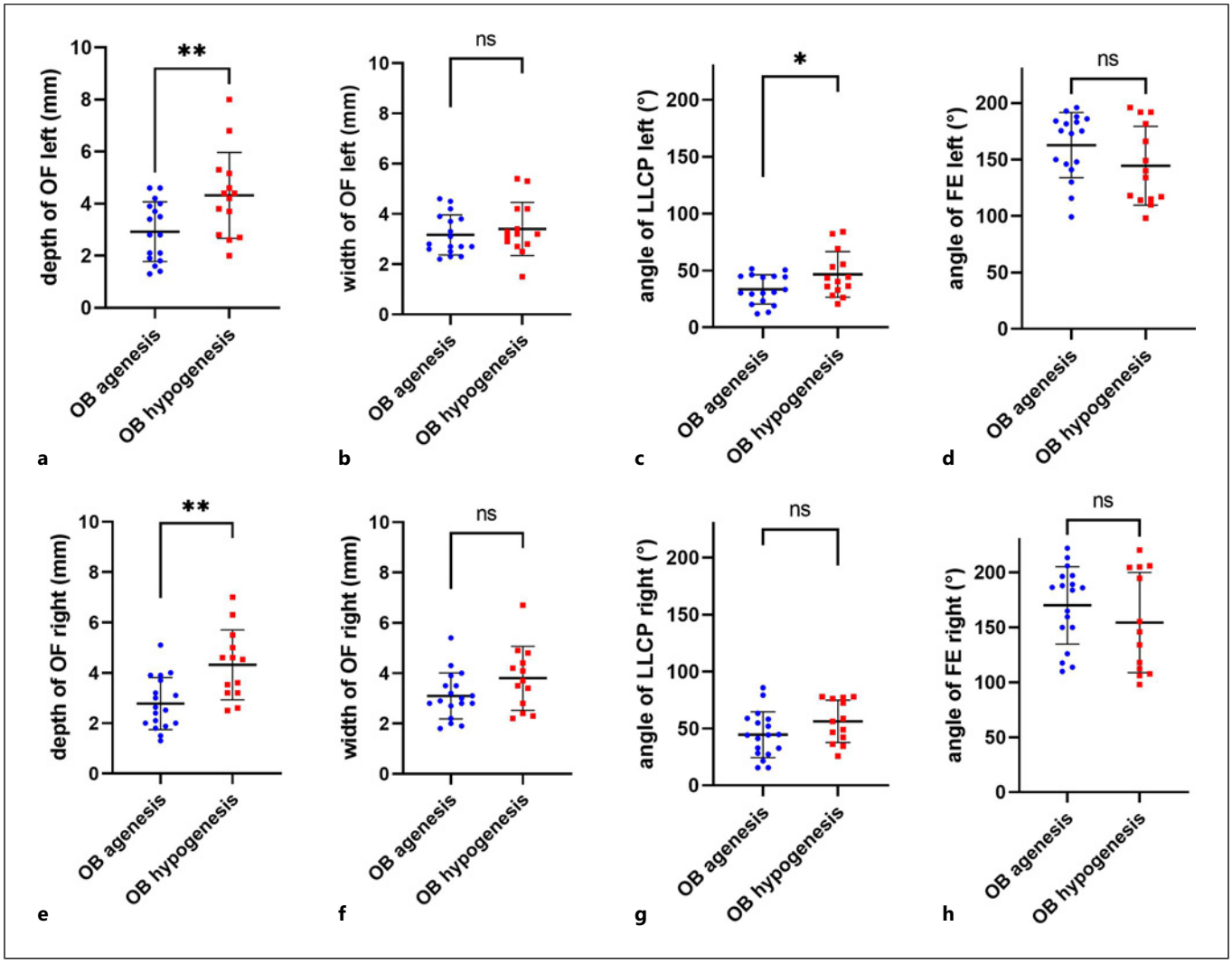

Fig. 5. Structures of the anterior skull base in ICA group according to the OB status and sides with OB agenesis and ICA with OB hypogenesis. **a**, **e** Mean of the depth of OF for OB agenesis and OB hypogenesis at both sides. **b**, **f** Mean of the width of OF for OB agenesis and OB hypogenesis at both sides. **c**, **g** Mean of angle of LLCP OB agenesis and OB hypogenesis at both sides. **d**, **h** Mean of angle of FE for OB agenesis and OB hypogenesis at both sides. FE, fovea ethmoidalis; LLCP, lateral lamella of the cribriform plate; OF, olfactory fossa; L, left; R, right. *$p < 0.05$, **$p < 0.01$, ns: $p > 0.05$.

common (57%), followed by type I (42%) and type III (1%). Gera et al. [22], in a study of 190 adult participants, observed that Keros type II was most frequent (65%), followed by type I (20%) and Keros type III (15%), with a mean depth of 5.4 mm. Meloni et al. [24] determined the depth of the cribriform plate to be 5.9 mm on average (range 1.3–17 mm). Also, in our healthy sample, a higher frequency of Keros type II (63%) was found; 33% were classified as type I, and 3% were type III. In our study, the mean depth of the OF was 4.7 mm at the right side and 4.9 mm at the left side, which is very similar to previous reports. However, individuals with ICA had a shallower OF; Keros type I (66%) is the most common, with an average depth of 3.4 mm.

In the present study, asymmetry in the depth of the cribriform was found in 12% of the cases. In addition, the width of the OF in ICA was significantly lower than in matched controls. Prior observations by Keros suggested that the average width of the OF is 2.1 mm in the anterior portion and that it gradually widens to 4.2 mm towards the posterior part. This was confirmed by Güldner et al. [25] who observed a mean width of the OF of 2.0 mm in

the anterior part and 3.25 mm in the posterior part. The present finding suggests that individuals with ICA have a significantly different anatomic structure of the OF than normosmic controls.

We further observed a significant difference between individuals with ICA and matched healthy individuals in the slope of the anterior skull base. In our sample with ICA, the FE had an average angle of 163° at the right side and 154° at the left side. However, in the control group, the FE was found with an average angle of 122° at the right side and 127° at the left side. In the literature review, few studies were found which reported a flattened FE. Lebowitz et al. [17] analyzed the flattening of the FE on 200 CT scans and observed 23% at the right side and 25% at the left side. Souza et al. [26], in a review of 200 CT scans, reported that flattening of the FE occurred in 19% on the right and 30% on the left. However, these studies did not quantitatively evaluate the angle of the FE as defined in this study. Angle of the LLCP, formed by the LLCP and horizontal line, can also be used to describe the slope of the anterior skull base. Data from 150 CT scans of healthy individuals show that the mean degree of the angle of the LLCP was 70.1°, ranging from 28 to 88° [27]. This is in line with the finding of Gera et al. [22] who observed that the mean degree of the angle of the LLCP was 71.7°, ranging from 27 to 89°. Interestingly, the current study found that the mean angle in ICA is 39°, which appears to fall outside the normal range in matched controls and healthy participants from previous studies. Hence, individuals with ICA exhibit a more pronounced slope of the anterior skull base.

Several studies investigated the relationship among these morphological features of the anterior skull base. The depth of the OF is associated with the angulation of the LLCP [22, 26]. However, one study reported that there was no significant correlation between the depth of the OF and the angle of the LLCP [27]. In addition, the length of the LLCP was negatively correlated with the length of the FE and the angle of the LLCP [22]. Further, the angulation of the lateral lamella is also related to asymmetry of the FE [26]. In our study, significant correlations among morphological parameters of the anterior skull base were found both in ICA participants and the healthy group (Fig. 4).

As opposed to the lack of research on skull abnormalities in ICA, relatively more is known about the association between the brain structure and congenital olfactory deficits [28]. Distinct features include aplastic or hypoplastic OB and tract. Several studies showed a significantly shallower olfactory sulcus in ICA, believed to be a direct consequence of an increased thickness of corresponding cortex area (e.g., [14]).

The fact that individuals with ICA characterized by small or absent OBs clearly show altered skull base in the present study raises interesting questions about the integrated development of the brain and skull, and especially the OB and the surrounding bony structures. Similar to our finding that the structure of the anterior skull base can reflect the presence of an OB, studies on eyeballs show that the size of the orbital reflects the size of the eye in adult humans [29]. A significant positive linear relationship was found between obit and eyeball volumes [30]. Anophthalmia (congenital absence of the eyes) is accompanied by hypoplasia of the orbit because the eyeball is considered to be the main endogenous factor stimulating the form of the orbital cavity [31]. From an evolutionary perspective, the prevailing notion is that, in humans, the morphology of the cranial base is tightly related to the brain size [4]. Primordial OB is present at 41 days of gestation [32]. The OBs can be recognized in prenatal MRI after 30 weeks of gestation [33]. The growth of the cranial base reaches approximately 87% by the age of 2 years and 98% by the age of 15 years [34]. The anterior skull base, which primarily consists of cartilage during the second fetal month, remains largely cartilaginous at birth and undergoes gradual ossification over the first 2 years of life [35]. By the age of 4 years, the anterior skull base is typically fully ossified [36]. The cribriform plate region, in particular, is considered to be quite stable in shape and size from age 4 [37]. However, there are few direct investigations regarding the exact signals and signaling sources crucial for the interplay between OB and the anterior skull base over the course of development. Generally, hypotheses regarding factors responsible for that skull morphogenesis have been proposed, which are mostly associated with brain pressure distribution during growth and development [2]. Collectively, based on our results, we can speculate that OBs play a pivotal role in developing and maintaining a normal structure of the anterior skull base.

Limitations

A limitation of this study is the absence of syndromic forms of congenital anosmia, such as Kallmann syndrome, various ciliopathies, and congenital insensitivity to pain, which is due to the retrospective cross-sectional study character. This assessment would help us make these anterior skull base abnormalities widely applicable. A second limitation is that we did not include genetic

diagnostics of the participants, due to the retrospective cross-sectional study character. This would have been interesting, especially when considering the differences in genetic deficits involved in the various forms of congenital anosmia (e.g., mutation in the cyclic nucleotide-gated gene CNGA2 [38]); genetic abnormalities are often associated with morphogenetic processes, resulting in altered patterns of the skull base. A potential limitation of our study is the reliance on thorough medical histories for the diagnosis of ICA. As such, it is important to acknowledge that there may be a degree of uncertainty regarding the ICA status of the individuals who participated in our study, given that the diagnosis is primarily based on exclusion criteria.

Generalizability

A variety of congenital malformations of the skull may be encountered. Many clinical presentations – including hearing loss, impaired vision, cognitive disability, and mental disease – manifest in children or adults in association with such malformations [39–41]. Early detection of pathological changes and further differential diagnosis and therapy decisions are ascertained with evaluation of the skull. Standard MRI procedures allow for the noninvasive assessment of the skull, which showed perfect agreement with the results from direct measurements of the skull ($r > 0.99$) [42]. Our data showed that ICA is associated with morphological changes including not only the abnormality of OB – the current "gold standard" – but also changes in cranial bone structures, specific to the anterior skull base. This helps us further understand the pathophysiology of this developmental disorder. In addition, the present study supports the idea that the OB plays a role in the development of the anterior skull base.

Structural assessments of olfaction-relevant regions, e.g., the olfactory cleft, OB, anterior skull base, or cribriform plate, can be used to identify morphological differences when comparing these regions between patients and healthy controls. These morphological characteristics have been shown to be different in various causes of olfactory dysfunction, e.g., inflammation and idiopathic or traumatic olfactory loss [43–45]. They can also be used to advance our understanding of aging [46]. Assessment of the OB is recommended during the clinical investigation of participants with suspected congenital anosmia. Our study demonstrated that the bony structures surrounding the OB can help differentiate abnormalities from normal variation (ROC area was 0.70–0.80). It may add future additional complementary diagnostic insights for the assessment of congenital anosmia.

Although the configuration of the anterior skull base, like Keros classification, is generally assessed with CT imaging, which is not justifiable due to ionizing radiation concerns when we included healthy control, we instead used MRI to evaluate both the OB and surrounding bony structures, as the latter modality is superior for soft-tissue evaluation. A previous study had shown that MRI provides sufficient resolution to assess the anterior skull base [47]. Previous work showed that measurements of the skull performed on MR images are highly reliable and show an excellent agreement with CT-based measurements [48]. Thus, while the measurements that were employed in this study can be implemented on both CT and MRI scans, and CT scans may provide more detailed bony information, we believe that our MRI measurements are still valuable in assessing the overall morphology of the skull base in relation to OB defects. Our findings may be used in a clinical setting for the neuroradiological evaluation of individuals with ICA.

This approach may be of use in certain clinical situations where patients are not entirely sure whether or not they smelled anything in their lives, e.g., in children or in older participants who sometimes have difficulties reporting their symptoms adequately. In addition, the use of electrophysiological measures as an objective confirmation of the absence of olfactory function can be problematic because olfactory event-related potential measurements are not widely performed. Taking all that together, assessment of the morphology of the bony structures surrounding the OB provides an additional clue on the diagnosis in terms of the presence or absence of the olfactory function which may be useful for the diagnosis of ICA.

Despite these notable results, the sample of normosmic participant was rather small and it is not possible to state how frequent abnormal anterior skull base anatomy is in the normosmic population. Furthermore, it is worth mentioning that an abnormal OB or abnormalities of surrounding regions are not an absolute sign of congenital anosmia [49, 50]. Thus, although the presently described findings may predict congenital anosmia, this is certainly not always the case. We recommend the assessment of the anterior skull base in addition to – and not instead of – a detailed history collection and thorough olfactory testing.

Conclusion

This study provides baseline morphometric data of the anterior skull base in individuals with ICA. This is the first study to demonstrate that ICA participants have an

abnormal OB as well as an abnormal anterior skull base, characterized by a shallow OF and flattened ethmoid roof. This study supports the idea of an integrated development of OB and anterior skull base. These morphological patterns of the anterior skull base surrounding the OB are applicable in distinguishing individuals with ICA from normosmic controls and may therefore be useful for the diagnosis of ICA. However, given the absence of other common causes of congenital anosmia, the high degree of variation in the measurements and large overlap with the normosmic controls suggest that these findings should be interpreted with caution. Future studies with larger sample sizes and more comprehensive assessments of genetics are needed to validate and expand upon our results.

Acknowledgments

We are thankful to Maxime de Malherbe for providing MR images at very early stages of this project.

Statement of Ethics

This study protocol was reviewed and approved by the Medical Faculty Ethics Review Board, TU Dresden, approval numbers (EK348092018, EK235072018, EK96032015, EK 262082010). Written informed consent was obtained from participants to participate in the study. The research was conducted ethically in accordance with the World Medical Association's Declaration of Helsinki.

Conflict of Interest Statement

The authors have no conflicts of interest to declare.

Funding Sources

Thomas Hummel and Xiaoguang Yan are funded by the Technische Universität Dresden. Yun-Ting Chao would like to thank the MOST (Ministry of Science and Technology, Taiwan)/DAAD (German Academic Exchange Service) Sandwich Project (110-2927-I-010-504) for providing him with a scholarship to pursue research. The acquisition for validating images was also supported by MOST (108-2314-B-075-012).

Author Contributions

Xiaoguang Yan: conceptualization, methodology, data curation, formal analysis, writing – original draft preparation, and visualization; Hakim Benkhatar: conceptualization, data curation, and writing – review and editing; Yun-Ting Chao: data curation and writing – review and editing; Charalampos Georgiopoulos: writing – review and editing and visualization; Thomas Hummel: conceptualization, data curation, resources, writing – original draft preparation, writing – review and editing, supervision, project administration, and funding acquisition. All authors have read and agreed to the published version of the manuscript.

Data Availability Statement

All data generated or analyzed during this study are included in this article. Further inquiries can be directed to the corresponding author.

References

1 Olson EC, Miller RL. Morphological integration. Chicago: Univ.; 1958.
2 Moss ML, Young RW. A functional approach to craniology. Am J Phys Anthropol. 1960 Dec;18(4):281–92.
3 Neubauer S, Gunz P, Hublin JJ. Endocranial shape changes during growth in chimpanzees and humans: a morphometric analysis of unique and shared aspects. J Hum Evol. 2010 Nov;59(5):555–66.
4 Bruner E. Cranial shape and size variation in human evolution: structural and functional perspectives. Childs Nerv Syst. 2007 Dec;23(12):1357–65.
5 Bakken TE, Dale AM, Schork NJ. A geographic cline of skull and brain morphology among individuals of European Ancestry. Hum Hered. 2011;72(1):35–44.
6 Jellinger K, Gross H, Kaltenback E, Grisold W. Holoprosencephaly and agenesis of the corpus callosum: frequency of associated malformations. Acta Neuropathol. 1981;55(1):1–10.
7 Kallmann FJ, Schoenfeld WA, Barrera SE. The genetic aspects of primary eunuchoidism. Am J Ment Deficiency. 1944;48(3):203–36.
8 Pinto G, Abadie V, Mesnage R, Blustajn J, Cabrol S, Amiel J, et al. CHARGE syndrome includes hypogonadotropic hypogonadism and abnormal olfactory bulb development. J Clin Endocrinol Metab. 2005 Oct;90(10):5621–6.
9 Yousem DM, Geckle RJ, Bilker W, McKeown DA, Doty RL. MR evaluation of patients with congenital hyposmia or anosmia. AJR Am J Roentgenol. 1996 Feb;166(2):439–43.
10 Karstensen HG, Tommerup N. Isolated and syndromic forms of congenital anosmia. Clin Genet. 2012 Mar;81(3):210–5.
11 Hummel T, Landis BN, Rombaux P. Disrupted odor perception. Springer handbook of odor. Springer; 2017. p. 79–80.
12 Abolmaali ND, Hietschold V, Vogl TJ, Huttenbrink KB, Hummel T. MR evaluation in patients with isolated anosmia since birth or early childhood. AJNR Am J Neuroradiol. 2002 Jan;23(1):157–64.
13 Huart C, Meusel T, Gerber J, Duprez T, Rombaux P, Hummel T. The depth of the olfactory sulcus is an indicator of congenital anosmia. AJNR Am J Neuroradiol. 2011 Dec;32(10):1911–4.
14 Frasnelli J, Fark T, Lehmann J, Gerber J, Hummel T. Brain structure is changed in congenital anosmia. Neuroimage. 2013 Dec;83:1074–80.
15 Maione L, Benadjaoud S, Eloit C, Sinisi AA, Colao A, Chanson P, et al. Computed tomography of the anterior skull base in Kallmann syndrome reveals specific ethmoid bone abnormalities associated with olfactory bulb defects. J Clin Endocrinol Metab. 2013 Mar;98(3):E537–46.
16 Keros P. On the practical value of differences in the level of the lamina cribrosa of the ethmoid. Z Laryngol Rhinol Otol. 1962 Nov;41:809–13.

17 Lebowitz RA, Terk A, Jacobs JB, Holliday RA. Asymmetry of the ethmoid roof: analysis using coronal computed tomography. Laryngoscope. 2001 Dec;111(12):2122–4.
18 Hummel T, Whitcroft KL, Andrews P, Altundag A, Cinghi C, Costanzo RM, et al. Position paper on olfactory dysfunction. Rhinology. 2016 Jan;56(1):1–30.
19 Hummel T, Hummel C, Welge-Luessen A. Assessment of olfaction and gustation. Management of smell and taste disorders: a practical guide for clinicians. 1st ed. Stuttgart: Thieme; 2013. p. 58–75.
20 Oleszkiewicz A, Schriever VA, Croy I, Hahner A, Hummel T. Updated Sniffin' Sticks normative data based on an extended sample of 9,139 subjects. Eur Arch Oto-Rhino-Laryngol. 2019 Mar;276(3):719–28.
21 Hummel T, Pietsch H, Kobal G. Kallmann's syndrome and chemosensory evoked potentials. Eur Arch Oto-Rhino-Laryngol. 1991; 248(5):311–2.
22 Gera R, Mozzanica F, Karligkiotis A, Preti A, Bandi F, Gallo S, et al. Lateral lamella of the cribriform plate, a keystone landmark: proposal for a novel classification system. Rhinology. 2018 Mar;56(1):65–72.
23 Elwany S, Medanni A, Eid M, Aly A, El-Daly A, Ammar S. Radiological observations on the olfactory fossa and ethmoid roof. J Laryngol Otol. 2010 Dec;124(12):1251–6.
24 Meloni F, Mini R, Rovasio S, Stomeo F, Teatini GP. Anatomic variations of surgical importance in ethmoid labyrinth and sphenoid sinus. A study of radiological anatomy. Surg Radiol Anat. 1992;14(1):65–70.
25 Savvateeva DM, Guldner C, Murthum T, Bien S, Teymoortash A, Werner JA, et al. Digital volume tomography (DVT) measurements of the olfactory cleft and olfactory fossa. Acta Otolaryngol. 2010 Mar;130(3): 398–404.
26 Souza SA, Souza MMA, Idagawa M, Wolosker ÂMB, Ajzen SA. Análise por tomografia computadorizada do teto etmoidal: importante área de risco em cirurgia endoscópica nasal. Radiol Bras. 2008;41(3):143–7.
27 Abdullah B, Chew SC, Aziz ME, Shukri NM, Husain S, Joshua SW, et al. A new radiological classification for the risk assessment of anterior skull base injury in endoscopic sinus surgery. Sci Rep. 2020 Dec;10(1):4600.
28 Karstensen HG, Vestergaard M, Baaré WFC, Skimminge A, Djurhuus B, Ellefsen B, et al. Congenital olfactory impairment is linked to cortical changes in prefrontal and limbic brain regions. Brain Imaging Behav. 2018 Dec;12(6):1569–82.
29 Pearce E, Dunbar R. Latitudinal variation in light levels drives human visual system size. Biol Lett. 2012 Feb;8(1):90–3.
30 Pearce E, Bridge H. Is orbital volume associated with eyeball and visual cortex volume in humans? Ann Hum Biol. 2013 Dec;40(6):531–40.
31 Gundlach KK, Guthoff RF, Hingst VH, Schittkowski MP, Bier UC. Expansion of the socket and orbit for congenital clinical anophthalmia. Plast Reconstr Surg. 2005 Oct; 116(5):1214–22.
32 Muller F, O'Rahilly R. Olfactory structures in staged human embryos. Cells Tissues Organs. 2004;178(2):93–116.
33 Raybaud C, Barkovich AJ. Pediatric neuroimaging. Lippincott Williams & Wilkins; 2012.
34 Thiesen G, Pletsch G, Zastrow MD, do Valle CVM, do Valle-Corotti KM, Patel MP, et al. Comparative analysis of the anterior and posterior length and deflection angle of the cranial base, in individuals with facial Pattern I, II and III. Dental Press J Orthod. 2013; 18(1):69–75.
35 Belden CJ, Mancuso AA, Kotzur IM. The developing anterior skull base: CT appearance from birth to 2 years of age. AJNR Am J Neuroradiol. 1997 May;18(5):811–8.
36 Hughes DC, Kaduthodil MJ, Connolly DJA, Griffiths PD. Dimensions and ossification of the normal anterior cranial fossa in children. AJNR Am J Neuroradiol. 2010 Aug;31(7): 1268–72.
37 Afrand M, Ling CP, Khosrotehrani S, Flores-Mir C, Lagravère-Vich MO. Anterior cranial-base time-related changes: a systematic review. Am J Orthod Dentofacial Orthop. 2014 Jul;146(1):21–32.e6.
38 Karstensen HG, Mang Y, Fark T, Hummel T, Tommerup N. The first mutation in CNGA2 in two brothers with anosmia. Clin Genet. 2015 Sep;88(3):293–6.
39 Sepahdari AR, Zipser BD, Pakdaman MN. Imaging of congenital temporal bone anomalies. Operat Tech Otolaryngol Head Neck Surg. 2014 Mar;25(1):13–20.
40 Guercio JR, Martyn LJ. Congenital malformations of the eye and orbit. Otolaryngol Clin North Am. 2007 Feb;40(1): 113–40, vii.
41 Nagaishi M, Fujii Y, Sugiura Y, Suzuki K. Skull shape abnormalities in ischemic cerebrovascular and mental diseases in adults. Sci Rep. 2021 Sep;11(1):17616.
42 Cotton F, Rozzi FR, Vallee B, Pachai C, Hermier M, Guihard-Costa A-M, et al. Cranial sutures and craniometric points detected on MRI. Surg Radiol Anat. 2005 Mar; 27(1):64–70.
43 Schlosser RJ, Smith TL, Mace JC, Alt JA, Beswick DM, Mattos JL, et al. The Olfactory Cleft Endoscopy Scale: a multi-institutional validation study in chronic rhinosinusitis. Rhinology. 2021 Apr;59(2): 181–90.
44 Mahmut MK, Musch M, Han P, Abolmaali N, Hummel T. The effect of olfactory training on olfactory bulb volumes in patients with idiopathic olfactory loss. Rhinology. 2020 Aug;58(4):410–2.
45 Gudziol V, Marschke T, Reden J, Hummel T. Impact of anterior skull base fracture on lateralized olfactory function. Rhinology. 2020 Feb;58(1):45–50.
46 Ganjaei KG, Soler ZM, Mappus ED, Worley ML, Rowan NR, Garcia GJM, et al. Radiologic changes in the aging nasal cavity. Rhinology. 2019 Apr;57(2):117–24.
47 Saglam M, Salihoglu M, Tekeli H, Altundag A, Sivrioglu AK, Cayonu M. Is there an association between olfactory bulb volume and the Keros type of fossa olfactoria? J Craniofac Surg. 2014 Jul;25(4):1273–6.
48 Juerchott A, Freudlsperger C, Weber D, Jende JME, Saleem MA, Zingler S, et al. In vivo comparison of MRI- and CBCT-based 3D cephalometric analysis: beginning of a non-ionizing diagnostic era in craniomaxillofacial imaging? Eur Radiol. 2020 Mar;30(3): 1488–97.
49 Weiss T, Soroka T, Gorodisky L, Shushan S, Snitz K, Weissgross R, et al. Human olfaction without apparent olfactory bulbs. Neuron. 2020 Jan;105(1):35–45.e5.
50 Rombaux P, Mouraux A, Bertrand B, Duprez T, Hummel T. Can we smell without an olfactory bulb? Am J Rhinol. 2007 Oct;21(5): 548–50.